Energy and Buildings 41 (2009) 1051–1057

Contents lists available at ScienceDirect

Energy and Buildings

journal homepage: www.elsevier.com/locate/enbuild

Modelling the heat dynamics of building integrated and ventilated photovoltaic modules

Nynne Friling [a,*], María José Jiménez [b], Hans Bloem [c], Henrik Madsen [a]

[a] Informatics and Mathematical Modelling, Technical University of Denmark, Building 321, DK-2800 Lyngby, Denmark
[b] Department of Renewable Energies, Solar Energy in Buildings Project, CIEMAT, Madrid E-28040, Spain
[c] European Commisssion - Joint Research Centre, Building 45, I-21020 Ispra, Italy

ARTICLE INFO

Article history:
Received 10 March 2009
Accepted 22 May 2009

Keywords:
Continuous time systems
Stochastic modelling
Non-linear systems
Building integrated photovoltaic module (BIPV)
Heat transfer
Model recognition

ABSTRACT

This paper deals with mathematical modelling of the heat transfer of building integrated photovoltaic (BIPV) modules.

The efficiency of the photovoltaic (PV) module and its temperature are negatively correlated. It is therefore of interest to lower the temperature of the PV module by increasing the heat transfer from the PV module. The experiment and data originate from a test reference module the EC-JRC Ispra. The set-up provides the opportunity of changing physical parameters, the ventilation speed and the type of air flow, and this makes it possible to determine the preferable set-up.

To identify best set-up, grey-box models consisting of stochastic differential equations are applied. The models are first order stochastic state space models. Maximum likelihood estimation and the extended Kalman filter are applied in the parameter estimation phase. To validate the estimated models, plots of the residuals and autocorrelation functions of the residuals are analyzed.

The analysis has revealed that it is necessary to use non-linear state space models in order to obtain a satisfactory description of the PV module temperature, and in order to be able to distinguish the variations in the set-up. The heat transfer is increased when the forced ventilation velocity is increased, while the change in type of air flow does not have as striking influence. The residual analysis show that the best description of the PV module temperature is obtained when fins, disturbing the laminar flow and making it turbulent, are applied in the set-up combined with high level of air flow. The improved description by the model is mainly seen in periods with high solar radiation.

1. Introduction

The limitation in the world's oil resources requires the world economy to search for other resources. The introduction of renewable energy technologies, in particular solar energy in the built environment, will contribute significantly to reducing the dependency on fossil fuels. In this article a building integrated photovoltaic application is analyzed. The primary purpose of PV modules is generally to produce electricity and nowadays this is at an efficiency of 10–15%. Building integrated modules placed in facades can have a multiple functionality as a curtain wall that produces electricity, protects the building envelope and preheats air or water. This heated air or water can be used to supply heat to the indoor environment of the building.

Research has shown that the electrical efficiency and the temperature of the PV module are negatively correlated for building integrated polycrystalline silicon modules. The decrease in electricity production is 0.5%/ ° C for module temperatures above 25° C [5]. In order to reduce the heating of the PV module, natural or forced air ventilation behind the PV module could be applied.

In this article we consider an experimental set-up which aims to remove heat from the PV module and its boundaries while increasing electricity production.

The application of simulation tools is traditionally based on the application of several approximations such as standard surface heat transfer coefficients, tabulated values of the materials, etc. Although in many applications these simplifications lead to accurate enough results, there are other where more precise estimations are required to obtain appropriate representations of the simulated systems. The analysis applied in this paper is based on system identification that allows identification of realistic parameters, which given to simulation tools, can contribute to improving their performance. It can also provide empirical models to predict accurately the variables of interest.

Simple non-linear models for the dynamics related to the heat exchange of building integrated modules have been considered in

* Corresponding author. Fax: +45 4588 2673.
E-mail address: nynne@friling.dk (N. Friling).

0378-7788/$ – see front matter © 2009 Elsevier B.V. All rights reserved.
doi:10.1016/j.enbuild.2009.05.018

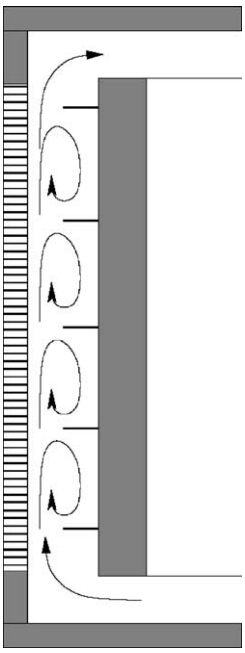

Fig. 1. The scheme of the test set-up with fins in the air gap [4].

[6,4]. In this article we will study in detail the influence of forced ventilation with fins in the air gap.

2. Experimental set-up

The experiment is set-up at the European Commission's Joint Research Centre in Italy and the data collected are from the period 30th July to 28th August 2002.

The test reference module is a 120 by 120 cm module consisting of 121 polycrystalline silicon based cells between two glass plates. The PV module is placed in an insulated box, where an air gap behind the PV module facilitates forced air flow, see Fig. 1. A detailed description of the set-up and data is found in [2].

The aim of the experiment is to investigate and describe how the change of conditions in the air gap behind the PV module influences the heat transfer by estimating the model on various data sets. Changing the conditions is also a way to test the reliability and strengths and weaknesses of previously formulated models.

The illustration in Fig. 1 shows the set-up where transversal fins are placed in the air gap. This makes it possible to modify the air resistance and turn the flow of air from laminar to turbulent. [3,1] Have shown that fins should lead to increased heat transfer. During the experiment the velocity of the forced air flow is also changed.

- The air resistance.

  Two set-ups are used in order to change the air resistance in the gap:

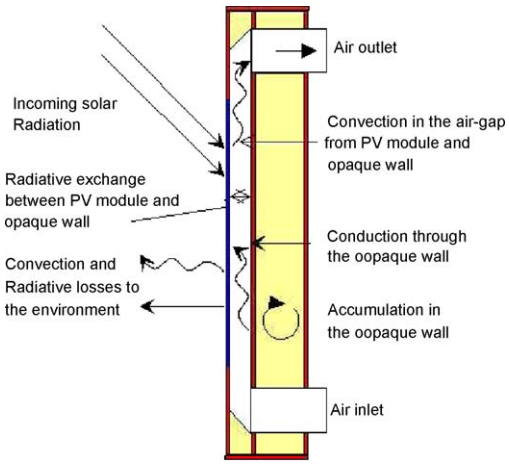

Fig. 2. Overview of the test set-up [2].

  - No fins resulting in an undisturbed laminar flow.
  - Fins creating a turbulent flow.
- The forced air velocity.

  The forced ventilation is held constant in a 24-h period. During the experiment two velocities are examined:
  - 2.49 m/s (level 10).
  - 3.43 m/s (level 13).

3. Data

The data is gathered at 1-min intervals from 00:00 to 23:59. Fig. 2 outlines the influencing heat transfers. Table 1 shows a list of the variables applied for this analysis.

The velocity of the forced air flow in the gap between the PV module and the wooden board is measured before and after the test by a Swema's Swemair 300 instrument which is based in a hot wire anometer. Fig. 3 shows plots of the PV module temperature and the irradiance, the two most influential variables. These two variables cannot be controlled in the experiment. It is, however, concluded that the levels of these input signals are of the same magnitude for all the series of data due to Fig. 3. The wind speed at the test area is seldom above 2 m/s.

4. Heat transfer

In the subsequent sections the temperature of the PV module will be considered as a state variable in the dynamical models, due to the fact that the efficiency of the PV module depends on the PV module temperature.

The heat transfer affecting the temperature of the photovoltaic module has the following contributions:

- Absorption of vertical solar radiation:

$$\alpha A I_v$$

Table 1
Measured data.

Signal	Symbol	Units	Comments
Time	t	min.	
Wind speed	W	m/s	Measured at the test site.
Ambient air temperature	T_{air}	°C	Measured by type T thermocouples.
Wood temperature	T_{wood}	°C	Temperature of backside cavity (middle). Measured by type T thermocouples.
Temperature difference	ΔT	°C	Temperature difference between in- and outlet of cavity measured by thermopile.
Irradiance	I_v	W/m^2	Global irradiance on PV module measured by a CM11 pyranometer near the test site.
Module temperature	T	°C	Measured temperature at the top of the PV module. Type T thermocouples are used.
Calculated temperature	T_m	°C	Temperature calculated from the models.

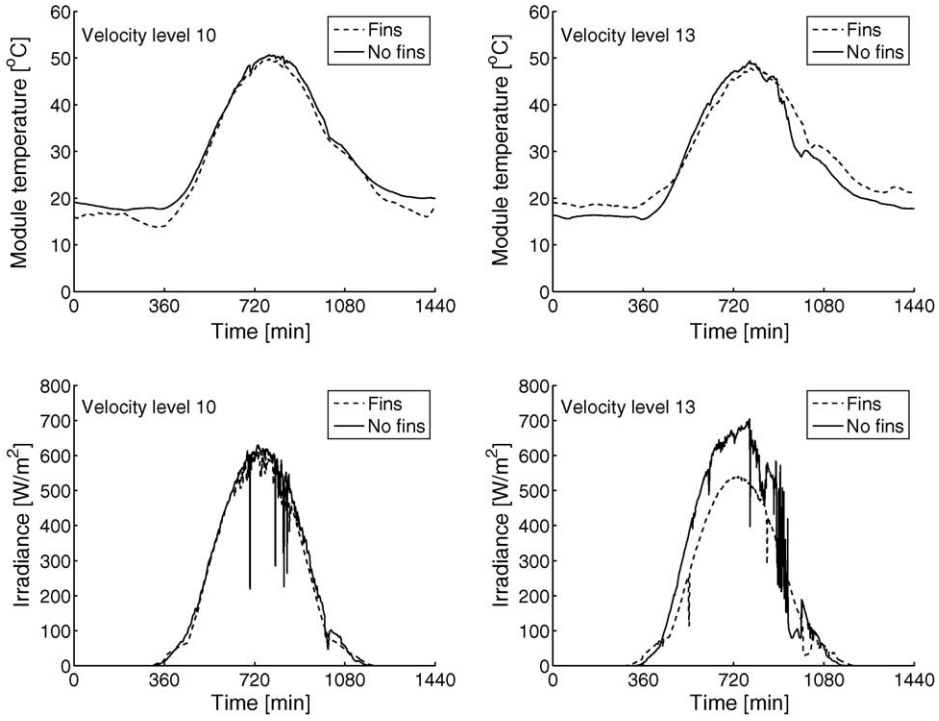

Fig. 3. Measured module temperature and irradiance.

- Infrared radiation to the surroundings:
  $\sigma\epsilon_{pv1}A(T^4 - T_{rad}^4)$
- Convection to the ambient air:
  $h_c(W)(T - T_a)$
- Infrared radiation to the wood wall:
  $\sigma(1/\epsilon_{pv2} + 1/\epsilon_w - 1)^{-1}A(T^4 - T_w^4)$
- Convection from the PV module to the air gap:
  $pw_{\text{gap}}S\rho c_p\Delta T$

Description of the variables and constants can be found in Table 1 and in the nomenclature. T_{rad} is the mean radiant temperature seen from the outdoor surface of the PV module. Note that the convection coefficient, $h_c(W)$, depends on the wind speed W. The above listed mechanisms for heat transfer will be applied to create the model in Section 6.1.

5. The modelling approach

The essential strength of the applied modelling framework is that prior physical knowledge can easily be combined with statistical information. This approach is called grey-box modelling. Stochastic differential equations, when used in the context of a continuous-discrete stochastic state space model, constitute a very natural framework for modelling realistic physical systems. It is furthermore possible to analyze non-linear phenomena and take advantage of prior physical knowledge, if available.

Data is collected in discrete time. It is, however, preferable to obtain a model in continuous time. The applied model consists of system equations, Eq. (1), in continuous time and the measurement equations, Eq. (2), in discrete time, i.e.

$$d\boldsymbol{x}_t = \boldsymbol{f}(\boldsymbol{x}_t, \boldsymbol{u}_t, t, \boldsymbol{\theta})\,dt + \boldsymbol{\sigma}(\boldsymbol{u}_t, t, \boldsymbol{\theta})\,d\boldsymbol{\omega}_t \tag{1}$$

$$\boldsymbol{y}_k = \boldsymbol{h}(\boldsymbol{x}_k, \boldsymbol{u}_k, t_k, \boldsymbol{\theta}) + \boldsymbol{e}_k \tag{2}$$

where $\boldsymbol{x}_t \in \mathcal{X} \subset \mathbb{R}^n$ is a vector of state variables, $\boldsymbol{u}_t \in \mathcal{U} \subset \mathbb{R}^m$ is a vector of input variables, $t \in \mathbb{R}$ is the time variable, $\boldsymbol{\theta} \in \Theta \subset \mathbb{R}^p$ is a vector of parameters, $\boldsymbol{y}_k \in \mathcal{Y} \subset \mathbb{R}^l$ is a vector of output variables. $\boldsymbol{f}(\cdot) \in \mathbb{R}^n$, $\boldsymbol{\sigma}(\cdot) \in \mathbb{R}^{n\times n}$ and $\boldsymbol{h}(\cdot) \in \mathbb{R}^l$ are possible non-linear functions; $\{\boldsymbol{\omega}_t\}$ is an n-dimensional standard Wiener process, and $\{\boldsymbol{e}_k\}$ is an l-dimensional white noise process with $\boldsymbol{e}_k \in N(\boldsymbol{0}, \boldsymbol{S}(\boldsymbol{u}_k, t_k, \boldsymbol{\theta}))$. $\boldsymbol{\sigma}(\cdot)$ is the gain of the increments of the Wiener process. It is assumed that $d\boldsymbol{\omega}_t$ and $\boldsymbol{e}_k$ are mutually uncorrelated.

5.1. Parameter estimation

Maximum likelihood estimation is applied to estimate the parameters of the model. The posterior probability density function for θ given in the observation, $\mathbf{Y}$, is given as:

$$p(\boldsymbol{\theta}|\mathbf{Y}) \propto \left(\prod_{i=1}^{S} \left(\prod_{k=1}^{N_i} \frac{\exp\left(-(1/2)(\boldsymbol{\epsilon}_k^i)^T (\boldsymbol{R}_{k|k-1}^i)^{-1} \boldsymbol{\epsilon}_k^i\right)}{\sqrt{det\left(|2\pi \boldsymbol{R}_{k|k-1}^i|\right)}} \right) \times p(\boldsymbol{y}_0^i|\boldsymbol{\theta}) \right) \tag{3}$$

S is a set of stochastically independent sequences and N_i is the number of observations in each sequence.

The maximum apsterior estimate is found as:

$$\hat{\boldsymbol{\theta}} = \arg\max_{\boldsymbol{\theta}\in\Theta}\{-\ln\left(p(\boldsymbol{\theta}|\mathbf{Y}, \mathbf{y}_0)\right)\} \tag{4}$$

The residual, $\boldsymbol{\epsilon}_k^i$, is calculated as $\boldsymbol{y}_k^i - \hat{\boldsymbol{y}}_{k|k-1}^i$. Due to the assumption that the conditional densities are Gaussian, the Kalman filter techniques can be used to estimate the conditional mean, $\hat{\boldsymbol{y}}_{k|k-1}^i$ and the associated covariance, $R_{k|k-1}^i$. However, since the models contain non-linearities, it is necessary to apply the extended Kalman filter [7]. The recursive algorithm of the extended Kalman filter consists of two main categories of equations: prediction and update. The update equations update the state predictions with the last measurement. A review of the theory of the extended Kalman filter is given in [11,7].

5.2. Statistical tests

The estimator in (4) also allows t-tests to be performed to test the hypothesis:

$$H_0: \quad \theta_j = 0 \tag{5}$$

against the alternative:

$$H_1: \quad \theta_j \neq 0 \tag{6}$$

for testing whether a given parameter θ_j is significant or not. The test quantity is the value of the parameter estimate divided by the standard deviation of the estimate, and under H_0 this quantity is asymptotically t-distributed with a number of degrees of freedom, DF, that equals the total number of observations minus the number of estimated parameters, i.e.:

$$z^t(\hat{\theta}_j) = \frac{\hat{\theta}_j}{\sigma_{\hat{\theta}_j}} \in t(\mathrm{DF}) = t\left(\left(\sum_{i=1}^{S}\sum_{k=1}^{N_i} l\right) - p\right) \tag{7}$$

where, if there are missing observations in $\boldsymbol{y}_k^i$ for some i and some k, l is replaced with the appropriate value of $\bar{l}$. To facilitate these tests, $z^t(\hat{\theta}_j)$, $j = 1, \ldots, p$, are computed along with the probabilities:

$$P(t < -|z^t(\hat{\theta}_j)| \wedge t > |z^t(\hat{\theta}_j)|), \quad j = 1, \ldots, p \tag{8}$$

More details about the statistical tests can be found in [10,11].

5.3. Model validation

It is important to test if the model describes the data and system satisfactorily. The residuals can be used for testing whether the model is adequate, since a representative model will lead to a sequence of residuals that behave as white noise. The residuals are mutually uncorrelated with mean 0 and constant variance, σ_ϵ^2. The residuals are analyzed in the time domain and test of the estimated autocorrelation function.

5.4. Software implementation

The models are estimated using the computer program CTSM, or Continuous Time Stochastic Modelling. CTSM has a grafical user interface, where it is possible to type in models as given in Eqs. (1) and (2) and estimate the optimal parameters. Guidance of how to obtain and use CTSM is found in [8,9].

6. The model

6.1. Non-linear model

The purpose of the applied model is to be able to describe and predict the temperature of the PV module, T_m. The applied model is first formulated in [6]. Prior research, [6,4], has shown that the description of the output variable is improved significantly when non-linear models are applied. A likelihood ratio test between a subset linear model and the current model underlined the necessity of applying this advanced non-linear model in order to obtain a satisfactory description.

The dynamics of the PV module temperature are formulated, in accordance to the heat transfer phenomena in Section 4, as:

$$\overbrace{C_{pv}\frac{dT}{dt}}^{\frac{J}{Ks}=W} = \overbrace{Ah_c W^{k_{airwind}}(T_{air}-T)}^{m^2\frac{W}{m^2K}K=W} + \overbrace{pw_{gap}S\rho c_p \Delta T}^{\frac{m}{s}m^2\frac{kg}{m^3}\frac{J}{kgK}K=W} + \overbrace{\frac{A\sigma}{(1/\epsilon_{pv_2})+(1/(\epsilon_w+1))}(T_{wood}^4 - T^4)}^{m^2\frac{W}{m^2K^4}K^4=W} + \overbrace{A\sigma\epsilon_{pv_1}(T_{rad}^4 - T^4)}^{m^2\frac{W}{m^2K^4}K^4=W} + \overbrace{A\alpha I}^{m^2\frac{W}{m^2}=W} + dw \tag{9}$$

$$T_m = T + e \tag{10}$$

In short (9) and (10) can be written as:

$$dT = k_{air}W^{k_{windair}}(T_{air} - T)\,dt + k_{delta}\Delta T\,dt + k_{wood}(T_{wood}^4 - T^4)\,dt + k_{rad}(T_{rad}^4 - T^4)\,dt + k_{irrad}I\,dt + dw \tag{11}$$

$$T_m = T + e \tag{12}$$

The state space model is outlined above in Eqs. (11) and (12). The model is established considering the three heat transfer phenomena: conduction, convection and radiation as described previously in Section 4. No conductive heat transfers are included in the model, since the thickness of the PV module can be neglected. The convective heat transfer terms represent the heat exchange with the ambient air and the temperature difference in the air gap. Two radiative influences are added in the model. First the heat transfer from the wooden board behind the PV module to the PV module. Secondly the long wave radiation which is assumed to be dependent on some mean radiant temperature, T_{rad}. This temperature is defined as an auxiliary parameter, representing the mean radian temperature seen from the outdoor surface of the PV module. It depends on the temperatures of ground, sky, and all surfaces surrounding the PV surface. T_{rad} is actually a variable, which has to be estimated like other parameters. [6,4] Report, that even considering this approximation, a model including this term gives better performance than analogous models not including it. The last term in the model is the contribution from the irradiance from the sun.

The non-linearities in the model are present in the radiative terms and the wind's influence on the heat transfer between the ambient wind and module.

6.2. The PV module temperature—the output variable

The mathematical model considered in (11) and (12) assumes a homogeneous temperature for the module. However, it is proven by thermal images, that the temperature is not homogeneous. Images from the period where data were collected are not available, but this non-homogeneity can be observed in Fig. 4 from different days. In practice the temperature of the PV module must be estimated from discrete measurement points. Consequently any temperature used as output is an approximation of the temperature of the PV module that must be chosen to be as representative as possible. [4] Reports a study based on residual analysis about the suitability of the temperature considered as output. The performance of the model is analyzed considering temperatures measured at different positions in the PV module and it is concluded that models considering the temperature

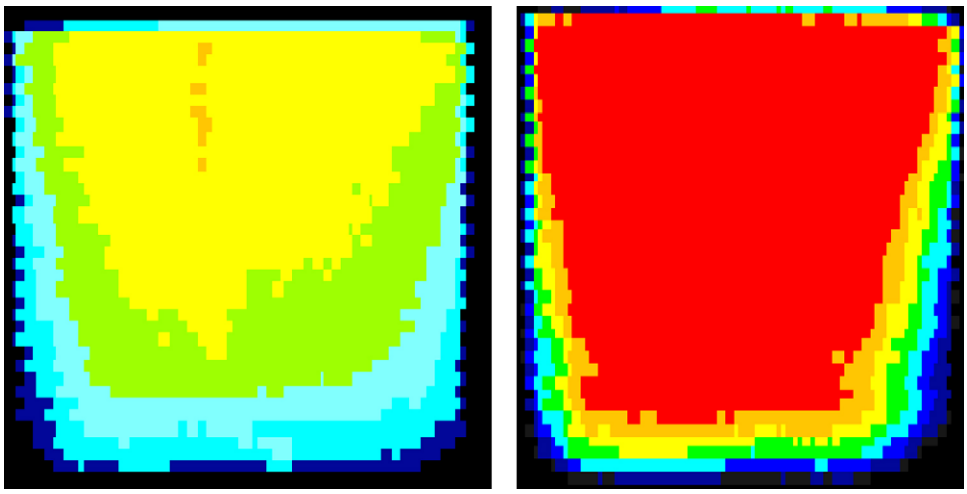

Fig. 4. Thermal images of the PV module taken at different days with different radiation.

measured at the top of the PV module show the best performance, so this temperature is considered as the output in the present paper.

7. Results

7.1. Model estimation

The model estimation is carried out for each of the four experimental conditions of the set-up. All the terms of the model (11) are proven to be significant by statistical testing. The standard deviations and averages of the residuals of the models are given in Table 2. A comparison of the values reveals that the standard deviations of the model based on data where the fins were installed show the lowest standard deviation overall. Moreover the standard deviation value in general increases along with increased level of velocity. Fig. 5 contains the residual plots for the four set-ups. The plots reveal that the model has most difficulties of prediction during periods of high radiation. The model has better performance on the data where the fins are placed in the air gap, which can be seen in Fig. 5, since the bulge during the periods of high radiation is not as remarkable. It is important to obtain good prediction during the periods of high radiation, since most of the electricity is produced in this time interval.

Table 2
Standard deviations and averages of the residuals.

Fins	Velocity	Average (std.dev.)
Yes	10	$-2.292 \times 10^{-4} (3.144 \times 10^{-2})$
	13	$2.206 \times 10^{-4} (3.423 \times 10^{-2})$
No	10	$-1.162 \times 10^{-4} (3.332 \times 10^{-2})$
	13	$-4.397 \times 10^{-5} (3.673 \times 10^{-2})$

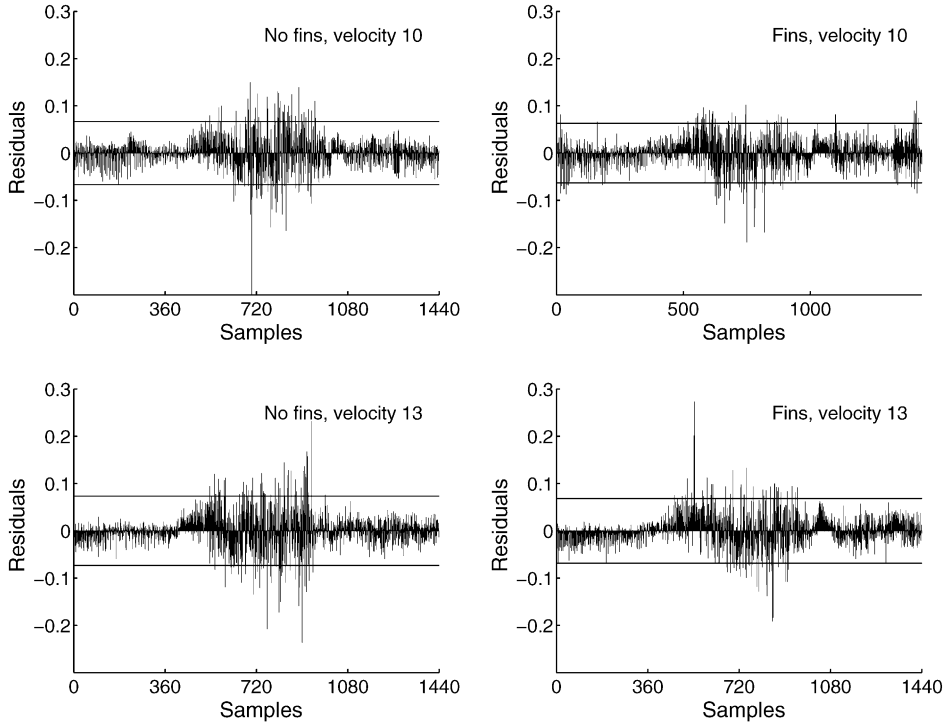

Fig. 5. Residual plots for forced velocity 10 without and with fins in the air gap.

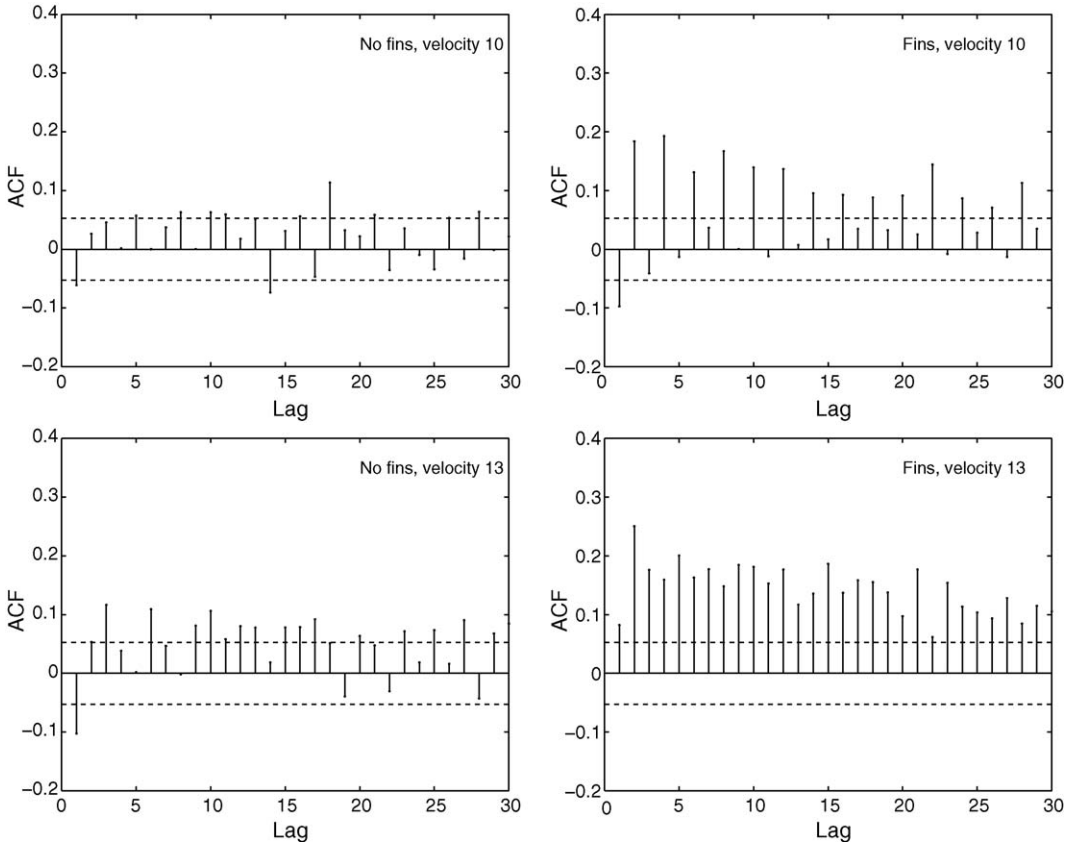

Fig. 6. The autocorrelation functions of the residuals of the estimated models.

The autocorrelation function plots of the residuals in Fig. 6 show that not all the autocorrelation functions behave as white noise. Even though not all the values are random and inside the 95% confidence intervals, the values are small. This means that only little information is left to describe.

7.2. The heat transfer of the BIPV module

Owing to the negative correlation between production of electricity and the temperature of the PV module, it is of interest to analyze the heat transfer from the PV module to the ambient air. Fig. 7 shows the estimated ambient convective coefficient, k_{air}, plotted against the wind speed raised to the power of the estimated coefficient, $k_{windair}$. The plot clearly shows that the velocity of the air in the gap has a strong influence on the heat transfer. The higher the forced velocity, the higher the heat transfer to the ambient air. The influence of the fins compared to the velocity level is small. The plot actually reveals that the heat transfer for the low velocity is higher when the fins are not included in the set-up, which is surprising. The influence in probably not significant. This difference becomes smaller the higher the forced air velocity becomes. For low wind speed the fins obviously acts as an insulation. At velocity level 13 the ambient convective coefficient is about the same for the set-up with and without the fins.

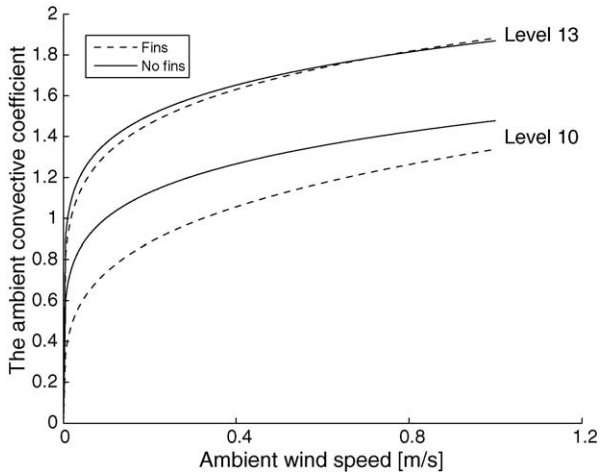

Fig. 7. The relationship between the ambient wind and the ambient convective coefficient for set-ups with or without fins. Also the forced velocity is varied.

8. Discussion

The method presented in this paper describes a powerful approach for modelling a stochastic non-linear physical system. Other modelling methods such as the frequently used RC-modelling is not able to handle non-linearities. Another advantage of the method is that knowledge of physical laws and statistically obtained information is combined. Furthermore statistical tests can help to reduce the model if some of the parameters tested are not significant. This is not possible by RC-modelling.

The aim of the modelling is to obtain a satisfactory description of the PV module temperature since the temperature is closely linked to the amount of electricity produced. The plots of the residuals indicate that the model has the biggest difficulties modelling the dynamics during the periods of high radiation.

The autocorrelation plots of the residuals indicate that the residuals are not white noise and that an extension of the model from single state model to a multiple state model might improve the performance of the model. On the other hand the potential to improve the model is limited, since only little variation is

undescribed. The thermal images show that the PV module temperature varies and therefore it could be beneficial to introduce a more advanced description of the output variable.

The results of the modelling are relatively sensitive to the measured wind speed. The ambient wind speed at the site where the data is gathered is light, seldom above 2 m/s. This can be a limitation of the scope of the model. During the modelling it was discovered that the parameters are also sensitive to the wind speed level. It would have been interesting to set up similar experiments in areas with higher wind speed. Until now no similar test set-ups have been tested at other locations. Data from other locations can help to test the applicability and reliability of the model.

9. Conclusion

The analysis has demonstrated that the non-linear single state model is able to describe the variations in the set-up. The heat transfer is increased when the forced ventilation level is raised. The effect of the fins is not as contributing, but it was discovered that the PV module temperature in general is lower when fins are installed in the air gap compared to the set-up where the forced ventilation is laminar. These results show that both the fins and a high forced velocity in the air gap together contribute to increased heat transfer from the PV module. This results in a higher production of electricity.

The analysis of the residuals of the model reveals that the best description is obtained when the fins are applied to the set-up. The difficulties of predicting during periods of high radiation are reduced. It can be concluded that the set-up including fins and high forced air velocity both in a physical and mathematical sense has the best performance. This results in the desired improved production of electricity due to the increased heat transfer from the PV module and the decrease in the temperature of the PV module.

Nomenclature

α	absorptance of the PV module
A	total surface area of the PV module
I_v	vertical global irradiance
ϵ_{pv1}	emissivity-exterior surface
ϵ_{pv2}	emissivity-interior surface
ϵ_w	emissivity of the wood surface
h_c	convective heat transfer coefficient
σ	Stefan–Boltzman constant
T	temperature of PV module
T_{air}	ambient air temperature
T_{rad}	mean radiant temperature
w_{gap}	air velocity in outlet tube
S	section of the outlet tube
ρ	air density
c_p	specific heat for air
ΔT	air temperature difference between inlet and outlet
p	fraction of energy to air from PV module

References

[1] F. Bazdidi-Tehrani, M. Naderi-Abadi, Numerical Analysis of Laminar Heat Transfer in Entrance Region of a Horizontal Channel with Transverse Fins, vol. 31, Elsevier, 2004, pp. 211–220.

[2] J.J. Bloem, Evaluation of a PV-integrated building application in a well-controlled outdoor test environment, Building and Environment 43 (2) (2007) 205–216.

[3] F.H.M. Christ, Comparison of measured and predicted data for PV hybrid systems, Master's thesis, University of Strathclyde Department of Mechanical Engineering, 2001.

[4] N. Friling, Stochastic modelling of building integrated photovoltaic modules, Master's thesis, Technical University of Denmark Informatics and Mathematical Modelling, 2006.

[5] IEC, IEC 61215 Crystalline Silicon Terrestrial Photovoltaic (PV) Modules—Design Qualifications and Type Approval, International Electrotechnical Commission, 2005.

[6] M.J. Jiménez, H. Madsen, H. Bloem, B. Dammann, Estimation of non-linear continuous time models for the heat exchange dynamics of building integrated photovoltaic modules, Energy and Buildings 40 (2) (2008) 157–167.

[7] N.R. Kristensen, H. Madsen, Continuous time stochastic modelling CTSM—mathematics guide, 2003, www2.imm.dtu.dk/ctsm.

[8] N.R.H. Kristensen, H. Madsen, S.B. Jørgensen, A method for systematic improvement of stochastic grey-box models, Computers and Chemical Engineering 28 (2004) 1431–1449.

[9] N.R.H. Kristensen, H. Madsen, S.B. Jørgensen, Parameter estimation in stochastic grey-box models, Automatica 40 (2004) 225–237.

[10] L. Ljung, System Identification: Theory for the User, second edition, Prentice-Hall, Upper Saddle River, USA, 1999.

[11] H. Madsen, Time Series Analysis, Chapman and Hall/CRC, New York, 2007.